RSC Advances

ROYAL SOCIETY OF CHEMISTRY

www.rsc.org/advances

Magnetic Beads Carrying Poly(Acrylic Acid) Brushes as "Nanobody Containers" for Immunoaffinity Purification of Aflatoxin B_1 from Corn Samples

Ying Xiong,[†,‡] Zhui Tu,[†] Xiaolin Huang,[†] Bing Xie,[§] Yonghua Xiong,[*†,‡] Yang Xu[†,‡]

[†]State Key Laboratory of Food Science and Technology, Nanchang University, Nanchang 330047, P. R. China

[‡]Jiangxi-OAI Joint Research Institute, Nanchang University, Nanchang 330047, P. R. China

[§]Centre of Analysis and Test, Nanchang University, Nanchang 330047, P. R. China

*Correspondence to:

Dr. Yonghua Xiong

State Key Laboratory of Food Science and Technology, and Jiangxi-OAI Joint Research Institute, Nanchang University

Address: 235 Nanjing East Road, Nanchang 330047, P.R. China

Phone: +0086-791-8833-4578. Fax: +0086-791-8833-3708.

E-mail: yhxiongchen@163.com.

Abstract:

The magnetic-bead-based immunoaffinity extraction (M-IAE) method has been widely used for the purification of aflatoxin B_1 (AFB_1) from complex food and feed matrices. However, this method suffers from several inherent disadvantages that limit its practical application, including low reusability and limited saturated adsorption capacity. Herein, we report an improved M-IAE for the highly efficient purification of AFB_1 from corn samples. This method involves the expression of anti-AFB_1 nanobodies (Nbs), which possess high degeneration resistance, to replace conventional antibodies; and magnetic beads carrying poly(acrylic acid) brushes (MB@PAA) were fabricated as an "Nb container" for improving AFB_1 adsorption capacity. The MB@PAA shows a high loading capacity for anti-AFB_1 Nbs at 623 μg/g, which is 19-fold the magnitude of that of conventional MB@Nbs. Meanwhile, the resultant MB@PAA@Nbs exhibit good AFB_1 adsorption, with a maximum adsorption capacity of 0.23 mg/g, which is 35-fold superior to that of the conventional MB@Nbs. MB@PAA@Nbs can be reused at least 10 times, without obvious loss of the capture efficiency for AFB_1. The reliability and practicability of the proposed MB@PAA@Nbs for AFB_1 extraction were further evaluated using AFB_1-spiked corn samples. In brief, the proposed MB@PAA@Nbs-based immunoaffinity extraction method is a highly promising, novel sample pre-treatment platform for AFB_1 as well as other mycotoxins.

Keywords: immunoaffinity extraction, magnetic beads, poly(acrylic acid) brushes, nanobodies, aflatoxin B_1.

1 Introduction

Mycotoxin contamination in food and feed materials has gained increasing attention as mycotoxin overexposure poses a potential threat to human and animal health.[1-3] Various analytical techniques, including high-performance liquid chromatography,[4] gas chromatography,[5] liquid chromatography coupled with mass spectrometry,[6] and enzyme-linked immunosorbent assay (ELISA),[7] have been developed for the sensitive determination of mycotoxins. In these methods, a proper pretreatment for the extraction and clean-up of mycotoxins is required to ensure the accuracy and sensitivity of the assay especially for the detection of trace amounts of analyte in a complex biological matrix.[8]

Several existing methods have been proposed for mycotoxin extraction and clean-up, such as liquid-liquid extraction (LLE), solid-phase extraction (SPE), molecular imprinted polymers (MIPs), and immunoaffinity extraction (IAE). LLE is a traditional method for mycotoxin extraction, which is based on the different solubilities of the toxin in two immiscible phases employed for the removal of background interferences. However, the process is time consuming and requires a large amount of organic solvent.[9] On the other hand, SPE technology has been widely used for mycotoxin sample pretreatment because of its high binding capacities and low cost. Nevertheless, this method lacks specificity and is easily affected by changes in the environment because using SPE cartridges for analyte extraction is mainly based on the differences in the chemical and physical properties of the analyte and the materials used.[10] Meanwhile, MIPs are tailor-made polymers with high selectivity for a given analyte. Nevertheless, the MIP method suffers from several shortcomings, such as polymer swelling in unfavorable solvents, slow binding kinetics of analytes, and potential sample contamination by template bleeding.[11,12] Antibody-based IAE is

considered as the most effective method for mycotoxin extraction and clean-up. But, this method is expensive because each column can only be used once. Moreover, immunoaffinity materials still require the filling of the column, which makes the operation process complicated and time consuming.[13-15]

By contrast, magnetic-bead-based IAE (M-IAE) exhibits many advantages over the traditional IAE. The magnetic adsorbent can interact homogeneously with the sample solution to achieve higher extraction efficiency. Furthermore, magnetic adsorbent can be performed in suspensions containing solid or oily components because of the application of an external magnetic field, which allows the rapid and convenient separation of analytes from these sample matrices.[16,17] Many efforts have been devoted to the application of M-IAE for the pre-concentration and clean-up of various mycotoxins, including ochratoxins,[18] zearalenone,[19] deoxynivalenol,[20] fumonisin B_1,[21] and aflatoxin B_1 (AFB_1).[22] However, the M-IAE method still possesses several inherent drawbacks that limit its popularization. These drawbacks include the method's low reusability and limited saturated adsorption capacity. Nanobodies (Nbs), which exhibit a unique antibody format naturally existing in the *Camelidae* species, are the smallest functional antigen-binding fragments.[23] Compared with conventional intact antibodies, Nbs possess many advantages including small size, high expression yield, and high stability even in extreme conditions, such as extremely low or high pH, high temperature, and organic solvent content.[24] These properties allow the wide application of Nbs in clinical diagnosis, medical therapy, food safety, and environmental monitoring.[25,26]

To our best knowledge, only a few investigations proposed the usage of Nbs instead of conventional antibodies in IAE for the pre-concentration and clean-up of mycotoxin. Herein, we report an enhanced M-IAE method to facilitate its practical

application. Aflatoxin B_1 was selected as the model analyte; it is a highly toxic mycotoxin and has been classified as a group I carcinogen by the International Agency for Research on Cancers.[27,28] To maximize the capture amounts of AFB_1, magnetic beads carrying poly(acrylic acid) brushes (MB@PAA) were synthesized and designed as "Nb containers" (MB@PAA@Nbs) for improving AFB_1 adsorption capacity. The Nb loading capacity and AFB_1 capturing efficiency of the resultant MB@PAA@Nbs were compared with carboxyl-modified magnetic beads. Moreover, the performance of MB@PAA@Nbs, including its reusability, reliability, and practicability, was further evaluated.

2 Experimental Section

2.1 Materials and reagents. N-(3-dimethylaminopropyl)-N′-ethylcarbodiimide (EDC), bovine serum albumin (BSA), and AFB_1 were purchased from Sigma-Aldrich Chemicals (St. Louis, MO, USA). Ethanethiol was obtained from J&K Chemicals. Acrylic acid (AA), 2, 20-azobisisobutyronitrile (AIBN), K_3PO_4, and $K_3PO_4{\cdot}H_2O$ were obtained from Aladdin Industrial Corporation (Shanghai, China). (4-(Chloro)phenyl)trimethoxysilane was purchased from Gelest, Inc. (Pennsylvania, America). Hydroxylated and carboxylated Fe_4O_3 nanoparticle doped magnetic silicon beads (HMBs and CMBs, respectively) and KBsphere™ Ni-IDA were purchased from Knowledge & Benefit Sphere Tech. Co., Ltd. (Suzhou, China). BCA Protein Quantitation Kit was purchased from Com Win Biotech Co., Ltd. (Beijing China). The commercial AFB_1 ELISA kit was provided by Wuxi Zodoboer Biotech. Co., Ltd. (Wuxi, China). The other reagents were of analytical grade or higher and were purchased from Sinopharm Chemical Corp. (Shanghai, China).

2.2 Synthesis of MB@PAA. As shown in Scheme 1A, HMBs carrying the poly(acrylic acid) brushes (MB@PAA) were synthesized via the surface-initiated reversible addition–fragmentation chain transfer (RAFT) polymerization method, including the synthesis of RAFT and free RAFT chain transfer agent (RAFT CTA and free RAFT CTA, respectively), the preparation of MB@RAFT, and the synthesis of MB@PAA. RAFT CTA and free RAFT CTA were synthesized according to a previously reported method.[29] MB@RAFT and MB@PAA were prepared through the following protocol. First, 59 μL of RAFT was added to a 13 mL ethanol solution containing 428 mg of HMBs. The mixture was refluxed under N_2 protection for 24 h. The resultant product was separated by magnetic shelf and washed with ethanol thrice. Yellow MB@RAFT (150 mg) was re-suspended with 10 mL of N,N-

dimethylformamide (DMF), and 3.24 g AA, 0.01 g AIBN, and 0.11 g free RAFT CTA were added to the DMF solution. Afterward, the mixture was transferred into a Schlenk tube. After five cycles of freeze–pump–thaw, the system was closed and incubated at 70 °C in an oil bath thermostat. After 3 h polymerization reaction, the MB@PAA was separated from the DMF solution and washed with ethanol for five times to fully remove impurities.

The Fourier-transform infrared (FTIR) spectra of the HMBs, MB@RAFT, and MB@PAA were obtained over the range of 400–4000 cm^{-1} using a Nicolet 5700 FTIR spectrometer (Thermo Fisher Scientific, Inc., USA). The carboxyl group density on the surface of the MB@PAA was determined as previously described,[30] with some modifications. Briefly, the electrode of an FE30 conductivity meter (Mettler Toledo, Shanghai, China) was immersed in 10 mL of ultrapure water containing 10 mg of MB@PAA. NaOH (0.1 M) was added dropwise under gentle stirring. The titration curve was plotted using the conductivity of the solution against the titrant volume of the NaOH solution. The carboxyl group density was calculated as $Ds = [(V_2 - V_1) \times C]/m$, where Ds (mmol/g) is the density of the carboxyl group on the MB@PAAs; V_1 and V_2 are the NaOH titrant volumes at the first and second inflection points of the titration curve, respectively; C is the concentration of the NaOH solution; and m is the mass of the MB@PAA. The thermogravimetric analysis (TGA) curves of MB@PAA@BSAs and CMB@BSAs were obtained from a simultaneous thermal analyzer (Perkin Elmer, USA). The morphologies of MB@PAA@BSAs and MB@PAA were determined using JEM-2100 scanning electron microscopy (SEM) (JEOL, Japan).

2.3 Expression and purification of anti-AFB_1 Nb. Phage particles carrying the anti-AFB_1 Nbs were obtained from an immune alpaca phage-display VHH library

constructed by our laboratory. The DNA fragment (G8) that coded for the anti-AFB_1 Nbs was cloned into the pET-25b (+) vector (Novagen, Billerica, MA, USA) and transformed into *Escherichia coli* Rosetta (DE3) cells to express soluble anti-AFB_1 Nbs. The single positive colony was inoculated into 5 mL LB medium containing 5% (v/v) glucose, 0.01% (v/v) ammonia benzyl, and chloramphenicol, and incubated at 37 °C overnight with shaking at 250 rpm. Then, 0.5 mL of the overnight culture was transferred to 50 mL of the LB medium for additional culture. When the culture reached OD_{600} = 0.6–0.8, 50 μL (0.1 mM) of isopropyl β-D-1-thiogalactopyranoside was added to induce the protein expression by culture for another 6 h. The cells were harvested by centrifugation at 5000 rpm for 10 min and then re-suspended with 10 mL PBS buffer for the ultrasonic cell-break. The protein supernatant was separated by centrifugation at 8000 rpm for 20 min. Anti-AFB_1 Nbs containing 6× His tag were purified with KBsphere™ Ni-IDA metal affinity column according to the manufacturer's instruction. The size of Nbs was assessed using sodium dodecyl sulfate polyacrylamide gel electrophoresis (SDS-PAGE) according to a standard protocol, followed by staining with Coomassie Brilliant Blue dye. The concentration of anti-AFB_1 Nbs was determined by the BCA Protein Quantitation Kit.

2.4 Preparation of MB@PAA@Nbs. The MB@PAA@Nbs conjugates were prepared according to the "chemical conjugation after electrostatic entrapment" (CCEE) method as previously described,[31] with some modification. In brief, 0.1 mg MB@PAA was suspended in 0.5 mL of 10 mM 2-(N-morpholino) ethanesulfonic acid buffer (MES) (pH = 5.0, containing 0.05 wt% Tween-20), and then 60 μg of anti-AFB1 Nbs was added at room temperature. After MB@PAA electrostatical adsorption of anti-AFB_1 Nbs for 15 min, 0.72 mg EDC was added for covalent coupling of the carboxyl group of MB@PAA with the amino group of Nbs at ambient

temperature for 2 h. The obtained MB@PAA@Nbs complex was separated by the magnetic shelf, washed with PBST buffer (PBS, pH = 7.4, containing 0.05 wt% Tween-20) for three times, and then stored in 0.2 mL PBS (containing 0.02% sodium azide) at 4 °C for further use. The binding efficiency of anti-AFB_1 Nbs onto the MB@PAA was evaluated by determining the amount of unbound anti-AFB_1 Nbs in the supernatant using the BCA Protein Quantitation Kit.

2.5 Adsorption behavior of MB@PAA@Nbs. The capture efficiency (CE), elution efficiency (EE), and adsorption isotherm behavior of MB@PAA@Nbs were evaluated through the following experiments. First, 0.1 mg of MB@PAA@Nbs was added into 0.5 mL PBS buffer containing 20% methanol with AFB_1 final concentrations from 2 ng/mL to 200 ng/mL and then incubated at room temperature with gentle shaking. After adsorption for 1 h, the MB@PAA@Nbs+AFB_1 complex was separated by magnetic shelf and washed with 20% methanol–PBS once. The bound AFB_1 onto the MB@PAA@Nbs was eluted by 200 μL pure methanol twice (100 μL each time). The AFB_1 concentrations in the supernatant and eluent were determined by a commercial ELISA kit. The CE of MB@PAA@Nbs was calculated according to the percentage fraction of those captured by MB@PAA@Nbs and the total AFB_1 spiked concentration as described by the equation CE (%) = $[(N - Nu) / N] \times 100\%$. On the other hand, EE was calculated according to the percentage fraction of those in the eluent and the total AFB_1 content by the equation EE (%) = $(Ne/N) \times 100\%$, where N is the total spiked AFB_1 content (ng), Nu is the unbound AFB_1 in the supernatant (ng), and Ne is the amount of AFB_1 in the eluent (ng/mL). The equilibrium adsorption capacity was calculated as $q_e = [(C_0 - Ce)V]/M$, where q_e (mg/g) is the equilibrium adsorption capacity; C_0 and Ce are the initial and equilibrium concentrations (mg/L), respectively, of AFB_1 in the adsorption solution

supernatant; V (L) is the volume of supernatant; and M (g) is the weight of the MB@PAA@Nbs.

2.6 Evaluation of the MB@PAA@Nbs. To evaluate the performance of MB@PAA@Nbs, the adsorption capacity of anti-AFB_1 Nbs onto MB@PAA and the CE of MB@PAA@Nbs for AFB_1 were compared with those of the CMBs and MB@Nbs, respectively. Briefly, 60 μg of anti-AFB_1 Nbs were coupled with 0.1 mg of MB@PAA and 1.0 mg of CMBs according to the CCEE method, respectively. The resultant MB@PAA@Nbs (0.1 mg) and MB@Nbs (1.0 mg) were used to capture 5 ng AFB_1 in 0.5 mL of PBS buffer containing 20% methanol. The recycling ability of MB@PAA@Nbs was performed by the evaluation of the CE of the MB@PAA@Nbs. Briefly, 0.1 mg of fresh MB@PAA@Nbs was used to capture 10 ng AFB_1 in the 0.5 mL absorption solution. After elution with pure methanol, the used MB@PAA@Nbs was regenerated in PBS buffer for over 12 h and then used for AFB_1 adsorption in the successive 10 independent experiments. In addition, the recovery and variable coefficient of MB@PAA@Nbs for AFB_1-spiked actual corn samples were used to evaluate the practicality of the proposed immuno-adsorption materials. The AFB_1 extraction and clean-up of corn samples using the MB@PAA@Nbs are illustrated in Scheme 1B. Briefly, 1.0 g of homogenized corn sample was mixed with 5.0 mL of 70% methanol using an ultrasonicator and then centrifuged at 8000 rpm for 10 min. The supernatant was centrifuged at 10000 rpm for another 5.0 min to discard the precipitate and then diluted threefold with ultrapure water. The MB@PAA@Nbs (0.1 mg) were added to 0.5 mL of the diluted extract. The mixture was then incubated at room temperature for 1 h. Subsequently, the MB@PAA@Nbs+AFB_1 complex was separated using an external magnetic field and

washed with 0.1 mL of PBS. The AFB_1 was eluted by 100 μL pure methanol twice (50 μL per each time), and the elution was kept at 4 °C for ELISA detection.

3 Results and discussion

3.1 Production of anti-AFB_1 Nbs. The DNA fragment that encoded anti-AFB_1 Nbs was amplified and cloned into a pET-25b (+) expression vector. Rosetta (DE3) was used as host strain for Nb expression. The expression of anti-AFB_1 Nbs was determined by a 15% SDS-PAGE. The results were shown in Figure S1, indicating that the anti-AFB_1 Nbs expressed were soluble proteins in the supernatant portion of the cell disruption. The molecular weight of the anti-AFB_1 Nbs is about 21 kDa. The recombinant anti-AFB_1 Nbs was purified using a KBsphere^{TM} Ni-IDA metal-affinity column. A nonspecific binding protein was washed with 50 mM imidazole solution, whereas the purified Nbs were eluted using 100 mM imidazole buffer. Protein concentration was measured using a BCA Protein Quantitation Kit, and the yield of the purified protein reached up to about 20.16 ± 0.26 mg/L of bacterial culture (purification yields are expressed as means ± standard deviation of three independent experiments).

3.2 Characterization of MB@PAA. MB@PAA was synthesized via a RAFT polymerization method. The FTIR spectra of HMB (Figure 1A) showed three typical absorption peaks of 585.24, 1098.72, and 3405.33 cm^{-1}, corresponding to the Fe–O, Si–O–Si, and Si–OH of Fe_3O_4 and SiO_2. After coupling with RAFT CTA, a characteristic signal at 632.521 cm^{-1} corresponding to the C–S stretching vibration was observed in the FTIR spectra of MB@RAFT. Two peaks at 2926.92 and 1722.46 cm^{-1} in the spectrum of MB@PAA represented the stretching vibration of the CH_2– and C=O bands that confirmed the modification of the PAA brushes. Moreover, the carboxyl group density on the resulting MB@PAA was determined by conductometric titration using a conductivity meter to measure signal changes. As shown in Figure 1B, the curve shows a good agreement with the mode of alkali

titrate–weak acid, and the carboxyl density is calculated to be 0.55 mmol/g MB@PAA. TGA analysis of MB@PAA@BSAs and CMB@BSAs was conducted, and results indicated that the protein loading capacity of MB@PAA largely improved compared with that of the CMBs (Figure 1C). The morphologies of the MB@PAA@BSAs and MB@PAA were determined using SEM. Figure 1D displays that the surface of MB@PAA is porous and relatively rough, whereas the surface of MB@PAA@BSAs became smoother with many collapses, indicating successful BSA conjugation.

3.3 Production of MB@PAA@Nbs. The anti-AFB_1 Nbs and MB@PAA conjugates were prepared using the "CCEE" method. For electrostatic entrapment, the pH value of the coupling buffer was considered as the most important factor that affects the adsorption efficiency of Nbs on the surface of MB@PAAs. The effect of buffer pH on Nb coupling efficiency was determined using 1.0 mg MB@PAA adsorption with 600 μg Nbs at the pH range of 4.0 to 6.0. Figure 2A indicates that the maximum Nb adsorption values were achieved at 400 ± 9 μg per mg MB@PAA in MES buffer at pH 5.0. Figure 2B shows the effect of EDC concentration on the coupling efficiency of the Nbs. The maximum Nb coupling amount was 424 ± 11 μg per mg MB@PAA at EDC concentration of 0.2 mM. Under the optimized coupling condition, the saturated labeling content of Nbs onto the MB@PAA was determined using 1.0 mg of MB@PAA conjugated with a series of amounts of anti-AFB_1 Nbs from 100 μg to 1.2 mg. As shown in Figure 2C, the maximum binding capacity of the Nbs for MB@PAA (1 mg) was achieved at 623 ± 23 μg, when 900 μg of anti-AFB_1 Nbs was coupled with 1 mg of MB@PAA. Moreover, the MB@PAA@Nbs containing different concentrations of anti-AFB_1 Nbs were used to capture the AFB_1, and the CE for AFB_1 was used to evaluate the reserved bioactivity of anti-AFB_1 Nbs on the surface of the

MB@PAA. Figure 2C indicates that the CE increased with increasing Nb content by 600 μg per mg MB@PAA and reached a maximum at 86.7% ± 4%. Subsequently, the CE of MB@PAA@Nbs for AFB_1 sharply decreased with the continual increase of Nb concentration. Thus, 600 μg anti-AFB_1 Nbs per mg MB@PAA was considered as the optimal amount of Nbs for the preparation of MB@PAA@Nbs. The Nb loading capacity and AFB_1 adsorption efficiency of MB@PAA@Nbs were further compared with those of carboxyl-modified magnetic beads. The results are shown in Figure 2D, which indicates that the adsorption capacity of MB@PAA for Nbs is about 19-fold higher than that of conventional CMBs, and the CE of MB@PAA@Nbs for AFB_1 is 35-fold higher than that of MB@Nbs.

3.4 Adsorption isotherm of AFB_1 on MB@PAA@Nbs. The equilibrium isotherm was obtained by capturing different concentrations of AFB_1 from 2.0 ng/mL to 200 ng/mL using 0.1 mg of MB@PAA@Nbs as absorbent materials at room temperature. Figure 3 indicates that the Langmuir equation is more appropriate to describe the adsorption behavior. The Langmuir equation is given by $C_e/q_e = 1/(K_L \times q_m) + C_e/q_m$, where q_m is the maximum adsorption capacity of MB@PAA@Nbs (mg/g), C_e is the equilibrium concentration of AFB_1 in solution (mg/L), q_e is the amount of AFB_1 adsorbed on the MB@PAA@Nb unit mass at equilibrium concentration (mg/g), and K_L is the Langmuir constant related to the affinity of the binding sites (L/mg). The linear curve of equilibrium isotherm is $C_e/q_e = 4.3103C_e + 0.0255$, which was obtained by plotting C_e against C_e/q_e ($R^2 = 0.9941$). The q_m and K_L were 0.23 mg/g and 196 L/mg, respectively. The higher correlation coefficient ($R^2 > 0.99$) indicates that the Langmuir isotherm is more suitable for the kinetics of AFB_1 adsorption because of the homogeneous and monolayer adsorption of the anti-AFB_1 Nbs.

3.5 Performance of MB@PAA@Nbs. To maximize the eluting AFB_1 from the MB@PAA@Nbs+AFB_1 complex, the percentage fraction of methanol in the elution buffer was optimized. Figure S2 shows that the EE of AFB_1 increased with increasing methanol concentration and reached a value of 89.85% ± 3.4% when 100% pure methanol was used as eluent. Therefore, 100% methanol is considered as the optimal methanol concentration for AFB_1 elution and used in the subsequent experiments. To estimate the reusability of the designed MB@PAA@Nbs, the CE of AFB_1 was measured through the repeated use of MB@PAA@Nbs for 10 times with 1 day intervals. Figure 4 shows that the CE of MB@PAA@Nbs for AFB_1 remains relatively high at 80.7% after the repeated use for 10 times, which had no significant difference with that of the first use ($p > 0.05$). This finding can be attributed to the superior properties of Nbs, especially the resistance to extreme environment.

The practicability of the MB@PAA@Nbs was evaluated by performing M-IAE using AFB_1-spiked corn samples. The recoveries of the intra- and inter-day assays were used to estimate the accuracy of the separation of the actual sample. Three AFB_1-spiked corn samples at concentrations of 5, 10, and 20 μg/kg were prepared for the intra- and inter-day assay precision analysis. Table 1 indicates that the average recoveries of the intra-day assay ranged from 96.4% to 104.4% with relative standard deviations (RSDs) of 2.3% to 11.0%, and the inter-day assay recoveries ranged from 95.7% to 103.6% with RSDs ranging from 5.8% to 9.0%. These above-mentioned results suggest that the MB@PAA@Nbs satisfy the requirements for the practical application of a simple and rapid AFB_1 clean-up.

4 Conclusions

We reported a new MB@PAA and anti-AFB_1 Nb nanocomposite (MB@PAA@Nbs) that can replace the conventional conjugates of MB and anti-AFB_1 antibody for AFB_1 separation. In this proposed nanocomposite, MB@PAA was used to increase the anti-AFB_1 Nb loading capacity through the PAA brushes, and the anti-AFB_1 Nbs were employed to replace the conventional intact antibody for rendering the reusability of the MB@PAA@Nbs complex due to its excellent properties, especially the resistance to extreme environment. The resulting MB@PAA (1 mg) shows a high loading capacity of 623 μg anti-AFB_1 Nbs at equilibrium state, which is 19-fold higher than that of the conventional MB without PAA brushes. By using the resultant MB@PAA@Nbs for the separation of AFB_1, the maximum adsorption capacity reaches to as high as 0.23 mg/g, which is 35-fold higher than that of conventional MB@Nbs. Moreover, the MB@PAA@Nbs can be reused for at least 10 times without obvious loss of CE. The reliability and practicability of the proposed MB@PAA@Nbs for AFB_1 separation were tested using AFB_1-spiked corn samples. Overall, the developed MB@PAA@Nbs-based IAE technology demonstrated great potential as a novel platform for the pre-treatment of other mycotoxins in food samples.

ASSOCIATED CONTENT

Supporting Information

The SDS-PAGE graph of anti-AFB_1 Nbs; Optimization of methanol concentration for AFB_1 elution. This material is available free of charge via the Internet at http://advances@rsc.org

AUTHOR INFORMATION

Corresponding Author

*(Y.X.) Phone: +0086-791-8833-4578. Fax: +0086-791-8833-3708. E-mail: yhxiongchen@163.com.

Address: 235 Nanjing East Road, Nanchang 330047, P.R. China.

Author Contributions

The manuscript was written through contributions of all authors. All authors have given approval to the final version of the manuscript. # These authors contributed equally to this work.

Notes

The authors declare no competing financial interest.

ACKNOWLEDGMENTS

This work was supported by a grant from the National Basic Research Program of China (2013CB127804), "Twelfth Five-Year Plan" for National Science and Technology Support Program (2013BAD19B02 and 2012BAK17B02), the Research Program of the State Key Laboratory of Food Science and Technology, Nanchang University (SKLF-ZZB-201306).

REFERENCE:

1 K. R. N. Reddy, B. Salleh, B. Saad, H. K. Abbas, C. A. Abel and W. T. Shier, *Toxin Reviews*, 2010, **29**, 3-26.

2 X. Liu, Y. Xu, Y. H. Xiong, Z. Tu, Y. P. Li, Z. Y. He, Y. L. Qiu, J. H. Fu, S. J. Gee and B. D. Hammock, *Analytical chemistry*, 2014, **86**, 7471-7477.

3 W. Xu, Y. Xiong, W. Lai, Y. Xu, C. Li and M. Xie, *Biosensors & bioelectronics*, 2014, **56**, 144-150.

4 Z. Dzuman, M. Zachariasova, Z. Veprikova, M. Godula and J. Hajslova, *Analytica chimica acta*, 2015, **863**, 29-40.

5 Y. Rodriguez-Carrasco, H. Berrada, G. Font and J. Manes, *Journal of chromatography. A*, 2012, **1270**, 28-40.

6 J. Rubert, N. Leon, C. Saez, C. P. Martins, M. Godula, V. Yusa, J. Manes, J. M. Soriano and C. Soler, *Analytica chimica acta*, 2014, **820**, 39-46.

7 C. N. Rossi, C. R. Takabayashi, M. A. Ono, G. H. Saito, E. N. Itano, O. Kawamura, E. Y. Hirooka and E. Y. S. Ono, *Food chemistry*, 2012, **132**, 2211-2216.

8 N. W. Turner, S. Subrahmanyam and S. A. Piletsky, *Analytica chimica acta*, 2009, **632**, 168-180.

9 P. D. Andrade, J. L. Gomes da Silva and E. D. Caldas, *Journal of chromatography. A*, 2013, **1304**, 61-68.

10 J. Rubert, C. Soler and J. Manes, *Talanta*, 2010, **82**, 567-574.

11 M. Szumski, D. Grzywinski, W. Prus and B. Buszewski, *Journal of chromatography. A*, 2014, **1364**, 163-170.

12 S. Wei, Y. Liu, Z. Yan and L. Liu, *RSC Adv.*, 2015, **5**, 20951-20960.

13 F. Ma, R. Chen, P. Li, Q. Zhang, W. Zhang and X. Hu, *Molecules*, 2013, **18**, 2222-2235.

14 W. J. Kong, S. Y. Liu, F. Qiu, X. H. Xiao and M. H. Yang, *The Analyst*, 2013, **138**, 2729-2739.

15 M. Vaclavikova, S. MacMahon, K. Zhang and T. H. Begley, *Talanta*, 2013, **117**, 345-351.

16 N. N. Lu, M. Xie, J. Wang, S. W. Lv, J. S. Yi, W. G. Dong and W. H. Huang, *ACS applied materials & interfaces*, 2015, **7**, 8817-8826.

17 M. Zhu, W. Liu, H. Liu, Y. Liao, J. Wei, X. Zhou and D. Xing, *ACS applied materials & interfaces*, 2015, **7**, 12873-12881.

18 P. Aqai, J. Peters, A. Gerssen, W. Haasnoot and M. W. Nielen, *Analytical and bioanalytical chemistry*, 2011, **400**, 3085-3096.

19 H.-J. Kim, S.-H. Kim, J.-K. Lee, C.-U. Choi, H.-S. Lee, H.-G. Kang and S.-H. Cha, *Journal of Veterinary Science*, 2012, **13**, 363.

20 H.-M. Lee, S.-O. Song, S.-H. Cha, S.-B. Wee, K. Bischoff, S.-W. Park, S.-W. Son, H.-G. Kang and M.-H. Cho, *Journal of Veterinary Science*, 2013, **14**, 143.

21 Y.-K. Wang, Y.-C. Wang, H.-a. Wang, W.-H. Ji, J.-H. Sun and Y.-X. Yan, *Food Control*, 2014, **40**, 41-45.

22 F. Xie, W. Lai, J. Saini, S. Shan, X. Cui and D. Liu, *Food chemistry*, 2014, **150**, 99-105.

23 S. Muyldermans, *Annual Review of Biochemistry*, 2013, **82**, 775-797.

24 T. He, Y. Wang, P. Li, Q. Zhang, J. Lei, Z. Zhang, X. Ding, H. Zhou and W. Zhang, *Analytical chemistry*, 2014, **86**, 8873-8880.

25 R. Chakravarty, S. Goel and W. Cai, *Theranostics*, 2014, **4**, 386-398.

26 I. Vaneycken, M. D'Huyvetter, S. Hernot, J. De Vos, C. Xavier, N. Devoogdt, V. Caveliers and T. Lahoutte, *Current opinion in biotechnology*, 2011, **22**, 877-881.

27 M. Ren, H. Xu, X. Huang, M. Kuang, Y. Xiong, H. Xu, Y. Xu, H. Chen and A.

Wang, *ACS applied materials & interfaces*, 2014, **6**, 14215-14222.

28 D. Tang, Y. Lin, Q. Zhou, Y. Lin, P. Li, R. Niessner and D. Knopp, *Analytical chemistry*, 2014, **86**, 11451-11458.

29 Z. Qu, F. Hu, K. Chen, Z. Duan, H. Gu and H. Xu, *Journal of colloid and interface science*, 2013, **398**, 82-87.

30 S. Kawaguchi, A. Yekta, and M. winnik, *Journal of colloid and interface science*, 1995, **176**, 362-368.

31 Z. Qu, K. Chen, H. Gu and H. Xu, *Bioconjugate chemistry*, 2014, **25**, 370-378.

Table

Table 1: Recovery efficiency of AFB_1 with MB@PAA@Nbs by ELISA in AFB_1 spiked corn samples.

AFB_1spiked corn sample (μg/kg)	Intra-day assay		Inter-day assay	
	Capture efficiency (%, n=3)	RSD (%)	Capture efficiency (%, n=3)	RSD (%)
5	104.4	2.3	98.4	9.0
10	96.4	8.5	103.6	7.5
20	99.2	11.0	95.7	5.8

Figure Captions:

Scheme 1. Schematic for MB@PAA@Nbs preparation and magnetic separation of AFB_1 with MB@PAA@Nbs

Figure 1. Characterization of materials: (A) FTIR spectrum of HMBs (a), MBs@RAFT (b), and MB@PAA (c); (B) conductometric titration graph of MB@PAA; (C) TGA graph of CMB-BSAs and MB@PAA@BSAs; (D) SEM micrograph of MB@PAAs and MB@PAA@BSAs.

Figure 2. Production of MB@PAA@Nbs and the outperform of MB@PAAs and MB@PAA@Nbs: (A) optimization of pH, (B) optimization of EDC concentration, (C) saturation binding of anti-AFB1 Nbs on MB@PAA and relationship between the adsorption amounts of anti-ANbs on MB@PAA and it's capture efficiency. Here, the additive amount of AFB_1 is 10 ng with 0.1 mg MB@PAA@Nbs in 0.5 mL 20% methanol-PBS solution. (D) outperform of MB@PAAs and MB@PAA@Nbs compared with conventional CMBs, the additive amount of AFB_1 is 5 ng with 0.1mg MB@PAAs and MB@PAA@Nbs, respectively, in 0.5 mL 20% methanol-PBS solution.

Figure 3. Adsorption isotherm and Langmuir model simulation (inset) for the adsorption of AFB_1 on MB@PAA@Nbs. Aqueous solution (0.5 mL) containing AFB_1 concentration from 2.0 ng/mL to 200 ng/mL and 0.1 mg MB@PAA.

Figure 4. Recycle times of MB@PAA@Nbs, the additive amounts of AFB_1 is 10 ng mixed with 0.1 mg MB@PAA@Nbs in 0.5 mL 20% methanol-PBS solution.

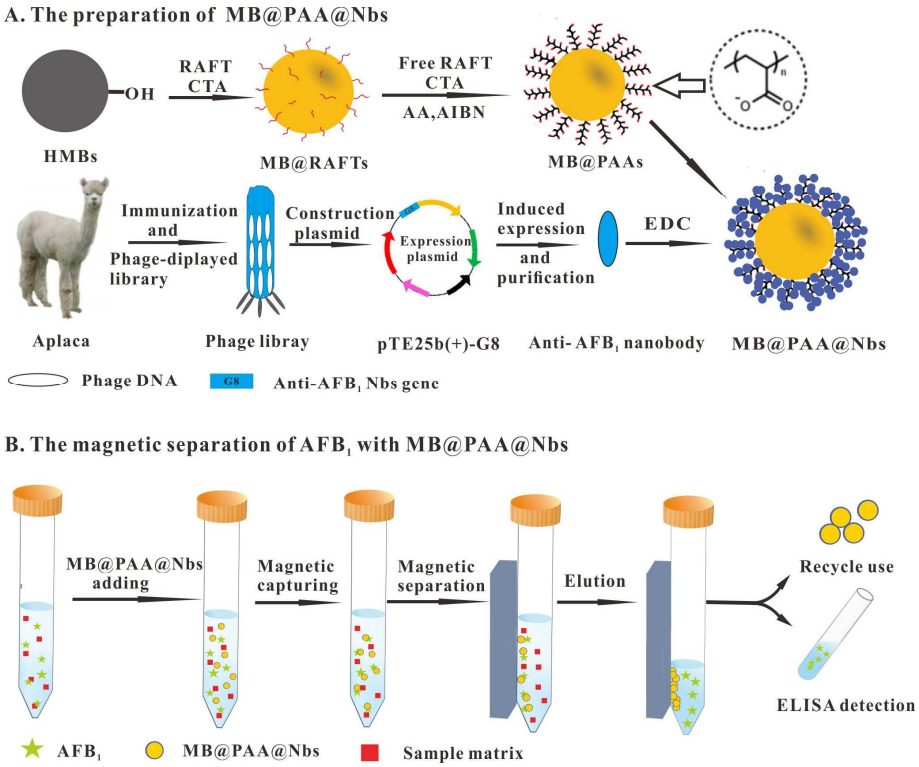

Scheme 1. Xiong *et al.*

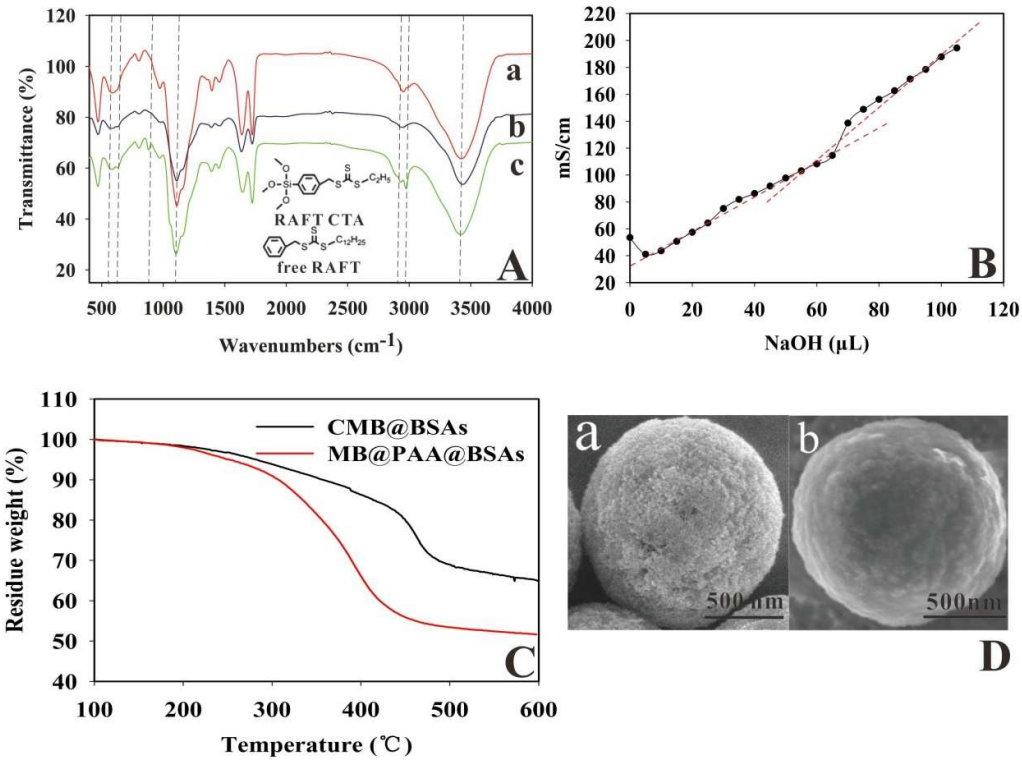

Figure 1. Xiong *et al.*

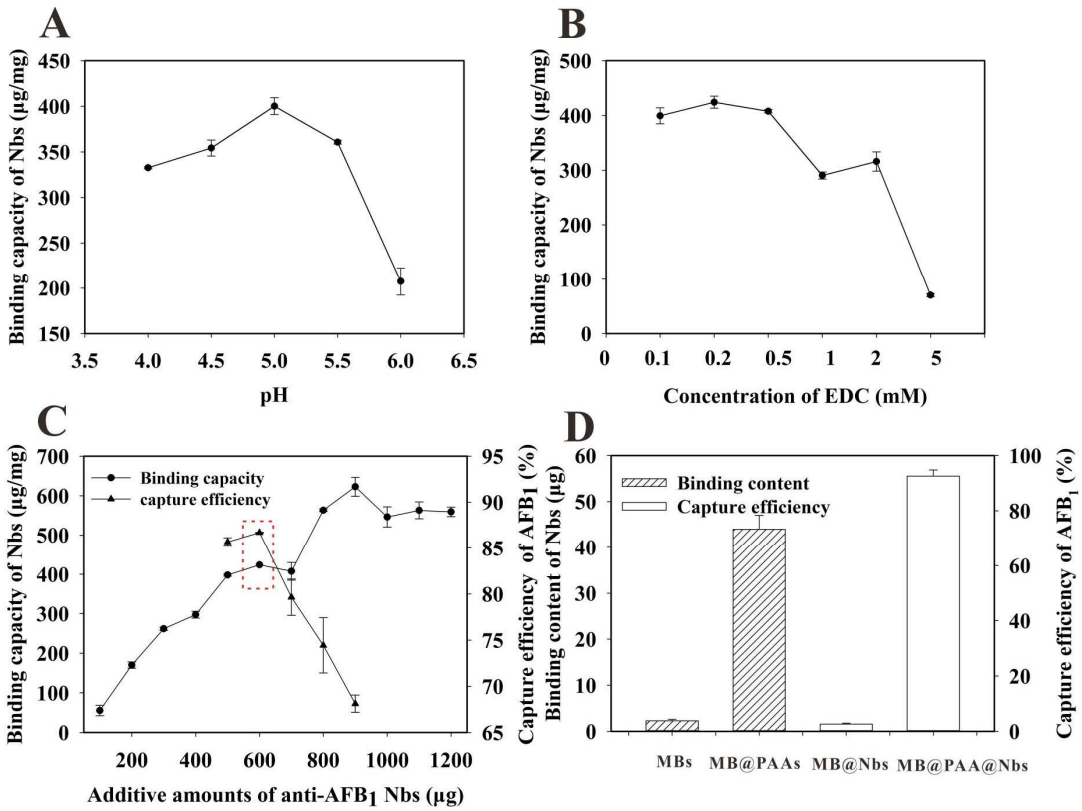

Figure 2. Xiong *et al.*

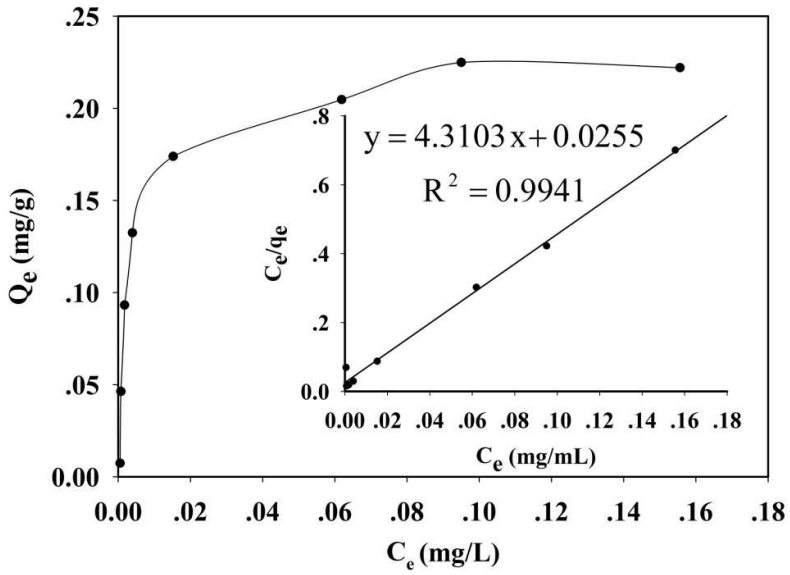

Figure 3. Xiong *et al.*

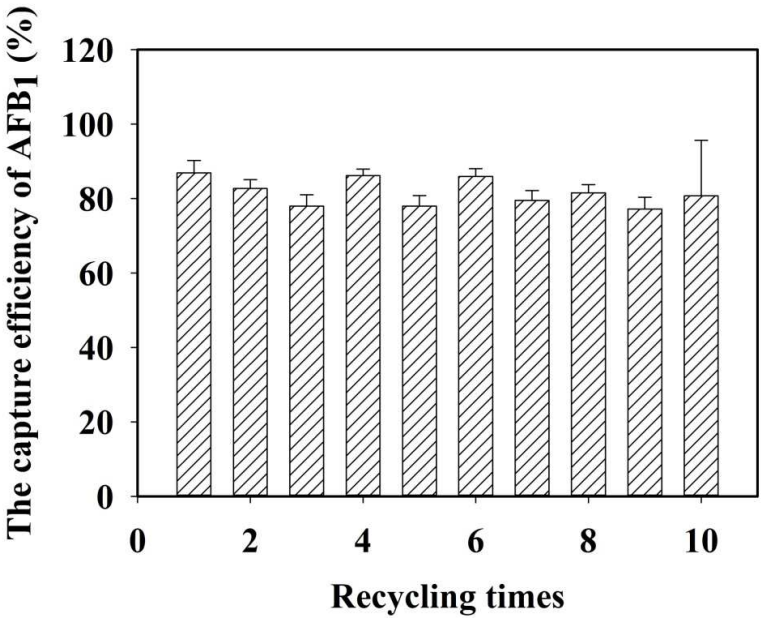

Figure 4. Xiong *et al.*